arXiv:1704.03060v1 [cond-mat.mtrl-sci] 10 Apr 2017

Correct Brillouin zone and electronic structure of BiPd

Alexander Yaresko,[1] Andreas P. Schnyder,[1] Hadj M. Benia,[1] Chi-Ming Yim,[2] Giorgio Levy,[3] Andrea Damascelli,[3] Christian R. Ast,[1] Darren C. Peets,[4] and Peter Wahl[2]

[1] *Max-Planck-Institut für Festkörperforschung, Heisenbergstr. 1, 70569 Stuttgart, Germany*
[2] *SUPA, School of Physics and Astronomy, University of St. Andrews, North Haugh, St. Andrews, Fife KY16 9SS, United Kingdom*
[3] *Department of Physics and Astronomy, University of British Columbia, Vancouver, British Columbia V6T 1Z1, Canada*
[4] *Advanced Materials Laboratory, Fudan University, Shanghai 200438, China*

A promising route to the realization of Majorana Fermions is in non-centrosymmetric superconductors, in which spin-orbit-coupling can lift the spin degeneracy of both bulk and surface bands. A detailed assessment of the electronic structure is critical to evaluate their suitability to host Majorana Fermions. Here we show that the interpretation of the electronic structure of the non-centrosymmetric superconductor BiPd reported by Neupane *et al.*[1] is based on a reciprocal unit cell which is not the actual Brillouin zone of the material, leading to an incorrect placement of the bands.

Recently, detailed photoemission characterizations of the electronic structure of BiPd have been published in three independent studies.[1–3] While the data broadly agree, the interpretation of the band structure does not. Neupane *et al*[1] and Setti *et al*[3] place all surface states at the Γ point, whereas Benia *et al*[2] locate those below the Fermi level at the S-point and those above the Fermi level at the Γ point, consistent with their calculations.[2,4] Clearly, these assignments cannot both be correct. A key difference is in the underlying unit cell used for calculations: Benia *et al.* use the primitive cell as reported by Ionov *et al.*[5] whereas Neupane and Setti use the larger, non-primitive unit cell reported by Bhatt *et al.*[6] Here we show that the two unit cells yield very similar band structures, but only if the correct Brillouin zone is used for the unconventional base-centered $B2_1$ structure of Bhatt [see Figure 1(a)]. Using the correct Brillouin zone places the surface bands in the occupied states at the S-point, whereas using a larger unit cell folds these bands to the zone center (Γ point).

A crystal structure's Brillouin zone is a uniquely-defined primitive cell in reciprocal space, while the reciprocal cell is a region in reciprocal space corresponding to the unit cell in real space. If the real space unit cell is a primitive cell, its reciprocal cell will correspond to the Brillouin zone. However, for convenience a unit cell is sometimes chosen to have alternative orientations, settings, or sizes, which affects the reciprocal cell but not the Brillouin zone. This is the case in α-BiPd, in which some authors chose a pseudo-orthorhombic supercell to aid comparison to related materials. In Figure 1(a) we show the reciprocal unit cell of α-BiPd for the larger pseudo-orthorhombic unit cell of Bhatt *et al.* and the primitive cell of Ionov *et al*, which is the correct Brillouin zone for both crystal structures. Experimentally, the correct choice of the unit cell can be verified from the size of the Brillouin zone: the reciprocal unit cell of the doubled cell is signficantly smaller than the Brillouin zone, with the X and Z points at $0.5\,\text{Å}^{-1}$ and $0.41\,\text{Å}^{-1}$, respectively. Comparison with ARPES constant energy maps [Figure 1(b)] confirms that features repeat on the scale of the Brillouin zone and not on the scale of the smaller reciprocal cell from Bhatt. Similarly, a surface reconstruction would lead to a smaller Brillouin zone than what is observed experimentally.

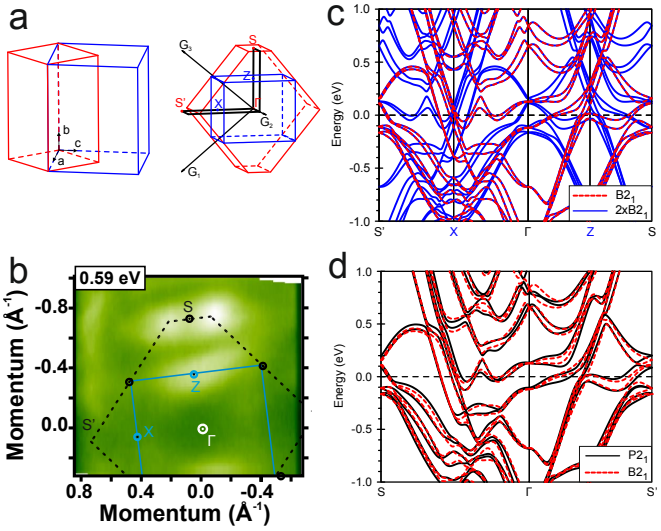

FIG. 1. Electronic structure in the monoclinic $P2_1$ and the pseudo-orthorhombic $B2_1$ unit cells. **a** Unit cell (left) and Brillouin zone (right) of the $P2_1$ unit cell (which is the same as for $B2_1$), the blue lines indicate the reciprocal unit cell for the doubled $B2_1$ unit cell as reported in Ref. 6. **b** Comparison of the Brillouin zone with ARPES data[2]. **c** Band structure for the reciprocal unit cell rather than the Brillouin zone, calculated for both $B2_1$ in its Brillouin zone (red dashed lines) and the reciprocal unit cell of the doubled unit cell (blue solid line). For the latter, X and Z are at the zone boundary. **d** shows the band structure in the same energy range as in **c** obtained in the Brillouin zone for both crystal structures, *i.e.* $B2_1$ (red dashed lines) and $P2_1$ (black solid lines).

Figure 1(c) shows the band structure calculated for the base-centered $B2_1$ unit cell defined by Bhatt *et al.* (red dashed lines) and for a doubled primitive pseudo-orthorhombic unit cell with the same lattice parameters and monoclinic angle. The electronic structure for the

doubled pseudo-orthorhombic cell shows twice as many bands as for the base-centered cell. Half of them exhibit exactly the same dispersion along X–Γ–Z as for the base-centered one, with additional bands being folded to Γ–X (Γ–Z) from S′–X (S–Z). This is to be compared with Supplementary Fig. 5 (right panel) of Neupane, showing excellent agreement. It is worth noting in addition that Setti *et al.* use an orthorhombic rather than a monoclinic unit cell, which is correct only for the high temperature phase β-BiPd. In Figure 1(d) we plot for comparison the band structure for unit cells of Bhatt and Ionov ($P2_1$), used by Benia *et al.*[2], on the same energy and momentum scale as in Fig. 1(c), which shows near-perfect agreement between bands for the two different crystal structures. It can be seen that using the correct Brillouin zone leads to a much smaller number of bands at the Γ point and preserves the directional band gap near the Γ point above the Fermi level.

The correct choice of the Brillouin zone is important for a number of reasons: (1) the marked anisotropy of the surface state at the S point is difficult to understand if it were at the Γ point, (2) The surface state in the unoccupied states becomes merely a surface resonance if calculated in the larger unit cell due to bands being folded to the Γ point. (3) A reliable assessment of the topological nature of the material is not possible without correct assignment of the time reversal invariant momenta. This is true in particular for the directional band gap at the Γ point, which is opened by spin-orbit coupling and is central to the topological nature of BiPd.

The confusion over the correct unit cell may stem from early reports which identified the structure as $Ccm2_1$, later refined to C_2^2 ($B2_1$) by Bhatt, a choice which facilitates comparison to the crystal structure of thallium(I) iodide (TlI)[6,7] — this, however, is not a primitive cell. More recent characterization by x-ray diffraction has identified the primitive unit cell as being of $P2_1$ symmetry, though the report is not available online.[5] To aid future work on BiPd, the structure refinements are reproduced here in Appendix A.

In conclusion, a correct treatment using the Brillouin zone rather than the reciprocal unit cell places the topologically-protected surface states below the Fermi level of the [010] and [0-10] surfaces near the S point, whereas the one above the Fermi level resides in a directional band gap opened by spin-orbit coupling at the zone center. The correct location of the surface states is crucial for understanding the physics in this material.

Methods: We employed fully relativistic linear muffin tin orbital calculations using the crystal structures by Bhatt and Ionov. ARPES was performed using a Helium-I source with a hemispherical SPECS HSA3500 electron analyzer. Details of the calculations have been reported in Refs. 2 and 4.

Author contribution statement: AY performed band structure calculations, HMB and CA measured ARPES on crystals grown by DCP, PW and DCP wrote the initial draft of the correspondence, all authors discussed and contributed to it.

Competing financial interests: The authors declare no competing financial interests.

[1] M. Neupane, N. Alidoust, M. M. Hosen, J.-X. Zhu, K. Dimitri, S.-Y. Xu, N. Dhakal, R. Sankar, I. Belopolski, D. S. Sanchez, T.-R. Chang, H.-T. Jeng, K. Miyamoto, T. Okuda, H. Lin, A. Bansil, D. Kaczorowski, F. Chou, M. Z. Hasan, and T. Durakiewicz, Nat. Commun. **7**, 13315 (2016), arXiv:1610.03431 [cond-mat.mes-hall].

[2] H. Benia, E. Rampi, C. Trainer, C. Yim, A. Maldonado, D. Peets, A. Stoehr, U. Starke, K. Kern, A. Yaresko, G. Levy, A. Damascelli, C. Ast, A. Schnyder, and P. Wahl, Phys. Rev. B **94**, 121407 (2016), arXiv:1608.01277 [cond-mat.mtrl-sci].

[3] S. Thirupathaiah, S. Ghosh, R. Jha, E. D. L. Rienks, K. Dolui, V. V. Ravi Kishore, B. Büchner, T. Das, V. P. S. Awana, D. D. Sarma, and J. Fink, Phys. Rev. Lett. **117**, 177001 (2016), arXiv:1609.08947 [cond-mat.supr-con].

[4] Z. Sun, M. Enayat, A. Maldonado, C. Lithgow, E. Yelland, D. C. Peets, A. Yaresko, A. P. Schnyder, and P. Wahl, Nat. Commun. **6**, 6633 (2015), arXiv:1407.5667 [cond-mat.supr-con].

[5] V. M. Ionov, N. A. Tomilin, A. E. Prozorovskii, A. N. Klimenko, Y. V. Titov, S. G. Zhukov, and G. V. Fetisov, Sov. Phys. Crystallogr. **34**, 496 (1989).

[6] Y. Bhatt and K. Schubert, J. Less-Common Met. **64**, P17 (1979).

[7] D. M. Kheiker, G. S. Zhdanov, and N. N. Zhuravlev, Zh. Eksp. Teor. Fiz. **25**, 621 (1953).

Appendix A: Reported Crystal Structures

Previously-reported crystal structures are reproduced here for reference, since most are not available online (or in English) at present.

TABLE I. Crystal structure of BiPd as refined by Kheiker[7], with lattice parameters $a = 7.203(1)$ Å, $b = 8.707(2)$ Å, and $c = 10.662(1)$ Å, in the space group $Ccm2_1$, an alternate setting of $Cmc2_1$ (No. 36).

Site	Wyckoff	x/a	y/b	z/c
Bi1	4a	0.108	0.	0.
Bi2	8b	0.125	0.274	0.722
Bi3	4a	0.650	0.	0.
Pd1	4a	0.108	0.	0.275
Pd2	8b	0.125	0.274	0.447
Pd3	4a	0.650	0.	0.275

TABLE II. Crystal structure of BiPd as refined by Bhatt[6], with lattice parameters $a = 7.200(1)$ Å, $b = 10.660(4)$ Å, $c = 8.708(2)$ Å, and $\beta = 89.70(3)^\circ$, in $B2_1$, an unconventional setting of $P2_1$ (No. 4). We have not reproduced the anisotropic thermal parameters here.

Site	Wyckoff	x/a	y/b	z/c
Bi1	2a	0.1193(6)	0.	0.9874(6)
Bi2	2a	0.6394(6)	0.9937(8)	0.0118(6)
Bi3	2a	0.1232(6)	0.7123(5)	0.2752(4)
Bi4	2a	0.6185(6)	0.7139(7)	0.2256(4)
Pd1	2a	0.086(1)	0.271(1)	0.001(1)
Pd2	2a	0.676(1)	0.265(1)	0.001(1)
Pd3	2a	0.146(2)	0.437(1)	0.260(1)
Pd4	2a	0.594(2)	0.441(1)	0.242(1)

TABLE III. Crystal structure of BiPd as refined by Bhatt[6] recalculated to conventional setting of $P2_1$ (No. 4), with lattice parameters $a = 5.635$ Å, $b = 5.664$ Å, $c = 10.660$ Å, and $\gamma = 100.83(3)^\circ$.

Site	Wyckoff	x/a	y/b	z/c
Bi1	2a	0.1319	0.1067	0.0
Bi2	2a	0.6276	0.6512	0.9937
Bi3	2a	-0.1520	0.3984	0.7123
Bi4	2a	0.3929	0.8441	0.7139
Pd1	2a	0.085	0.087	0.271
Pd2	2a	0.675	0.677	0.265
Pd3	2a	-0.114	0.406	0.437
Pd4	2a	0.352	0.836	0.441

TABLE IV. Crystal structure of α-BiPd at 293 K as refined by Ionov[5], with lattice parameters $a = 5.635(2)$ Å, $b = 5.661(2)$ Å, $c = 10.651(5)$ Å, and $\gamma = 100.85(3)^\circ$, in $P2_1$ (No. 4).

Site	Wyckoff	x/a	y/b	z/c	B (Å^2)
Bi1	2a	0.6565(6)	0.1055(6)	0.	0.6
Bi2	2a	0.1160(4)	0.6545(4)	0.0050(3)	0.4
Bi3	2a	0.6360(4)	0.6014(5)	-0.2116(3)	0.1
Bi4	2a	0.1129(6)	0.1529(5)	-0.2163(4)	0.7
Pd1	2a	0.406(1)	0.908(2)	0.235(1)	1.4
Pd2	2a	0.858(1)	0.346(1)	0.241(1)	0.3
Pd3	2a	0.598(1)	0.589(1)	0.068(1)	0.2
Pd4	2a	0.178(1)	0.191(1)	0.064(1)	0.8

TABLE V. Crystal structure of β-BiPd at 493 K as refined by Ionov[5], with lattice parameters $a = 5.674(2)$ Å, $b = 5.691(2)$ Å, $c = 10.596(4)$ Å, and $\gamma = 101.4(1)^\circ$, again in $P2_1$ (No. 4).

Site	Wyckoff	x/a	y/b	z/c	B (Å^2)
Bi1	2a	0.667(1)	0.142(2)	0.	1.1
Bi2	2a	0.143(4)	0.648(3)	0.034(1)	1.6
Bi3	2a	0.623(6)	0.589(5)	-0.166(2)	4.7
Bi4	2a	0.121(3)	0.109(2)	-0.213(1)	0.6
Pd1	2a	0.457(6)	0.950(5)	0.253(3)	1.4
Pd2	2a	0.857(2)	0.402(2)	0.222(2)	1.6
Pd3	2a	0.677(2)	0.673(2)	0.086(2)	1.7
Pd4	2a	0.107(2)	0.155(2)	0.039(1)	2.3